61 Color Constancy

DAVID H. BRAINARD

COLOR IS USED TO RECOGNIZE and describe objects. When giving directions, we might provide the detail that the destination is a yellow house. When judging the ripeness of a fruit, we might evaluate its color. The ability to perceive objects as having a well-defined color is quite remarkable. To understand why, it is necessary to consider how information about object spectral properties is represented in the retinal image.

A *scene* is a set of illuminated objects. In general, the illumination has a complex spatial distribution, so that the illuminant falling on one object in the scene may differ from that falling on another. Nonetheless, a useful point of departure is to consider the case where the illumination is uniform across the scene, so that it may be characterized by its *spectral power distribution*, $E(\lambda)$. This function specifies how much power the illuminant contains at each wavelength. The illuminant reflects off objects to the eye, where it is collected and focused to form the retinal *image*. It is the image that is explicitly available for determining the composition of the scene.

Object surfaces differ in how they absorb and reflect light. In general, reflection depends on wavelength, the angle of the incident light (relative to the surface normal), and the angle of the reflected light (Foley et al., 1990). It is again useful to simplify and neglect geometric considerations, so that each object surface is characterized by a *spectral reflectance function*, $S(\lambda)$. This function specifies what fraction of incident illumination is reflected from the object at each wavelength.

The light reflected to the eye from each visible scene location is called the *color signal*. For the simplified imaging model described above, the spectral power distribution of the color signal $C(\lambda)$ is readily calculated from the illuminant spectral power distribution and the surface reflectance function:

$$C(\lambda) = E(\lambda)S(\lambda) \quad (1)$$

The retinal image consists of the color signal incident at each location after blurring by the eye's optics. In the treatment here, such blurring may be safely ignored.

The imaging model expressed by equation 1 assumes that the light source is spatially uniform, that the objects are flat and coplanar, and that the surface reflectances are Lambertian. It is sometimes referred to as the *Mondrian World* imaging model. The assumptions of the Mondrian World never hold for real scenes. A more realistic formulation would include a description of the spatial distribution of the illuminant, the geometry of the scene, and how each object's spectral reflectance depends on the direction of the incident and reflected light (Foley et al., 1990; also see Fig. 61.2). Nonetheless, the Mondrian World is rich enough to provide a useful framework for initial analysis.

The form of equation 1 makes explicit the fact that two distinct physical factors, the illuminant and the surface reflectance, contribute in a symmetric way to the color signal. One of these factors, the surface reflectance, is intrinsic to the object and carries information about its identity and properties. The other factor, the illuminant, is extrinsic to the object and provides no information about the object.

Given that the color signal at an image location confounds illuminant and surface properties, how is it possible to perceive objects as having a well-defined color? Indeed, the form of equation 1 suggests that changes in illuminant can masquerade perfectly as changes in object surface reflectance, so that across conditions where the illuminant varies, one might expect large changes in the appearance of a fixed object. This physical process is illustrated by Figure 61.1. Each of the two patches shown at the top of the figure corresponds to a region of a single object imaged under a different outdoor illuminant. When the two patches are seen in isolation, their color appearance is quite different: there is enough variation in natural daylight that the color signal is substantially ambiguous about object surface properties.

When the two patches are seen in the context of the images from which they were taken, the variation in color appearance is reduced. This stabilization of appearance is by no means complete in the figure, where the reader views small printed images that are themselves part of a larger illuminated environment. For an observer standing in front of the home shown, however, the variation in perceived color is minimal and not normally noticed. This suggests that the visual system attempts to resolve the ambiguity inherent in the color signal by analyzing many image regions jointly: the full image context is used to produce a stable perceptual representation of object surface color. This ability is referred to as *color constancy*.

This chapter is about human color constancy. The literature on color constancy is vast, extending back at least to the eighteenth century (Mollon, in press), and this chapter does not attempt a systematic review. Rather, the goal is to provide an overview of how human color constancy can be studied

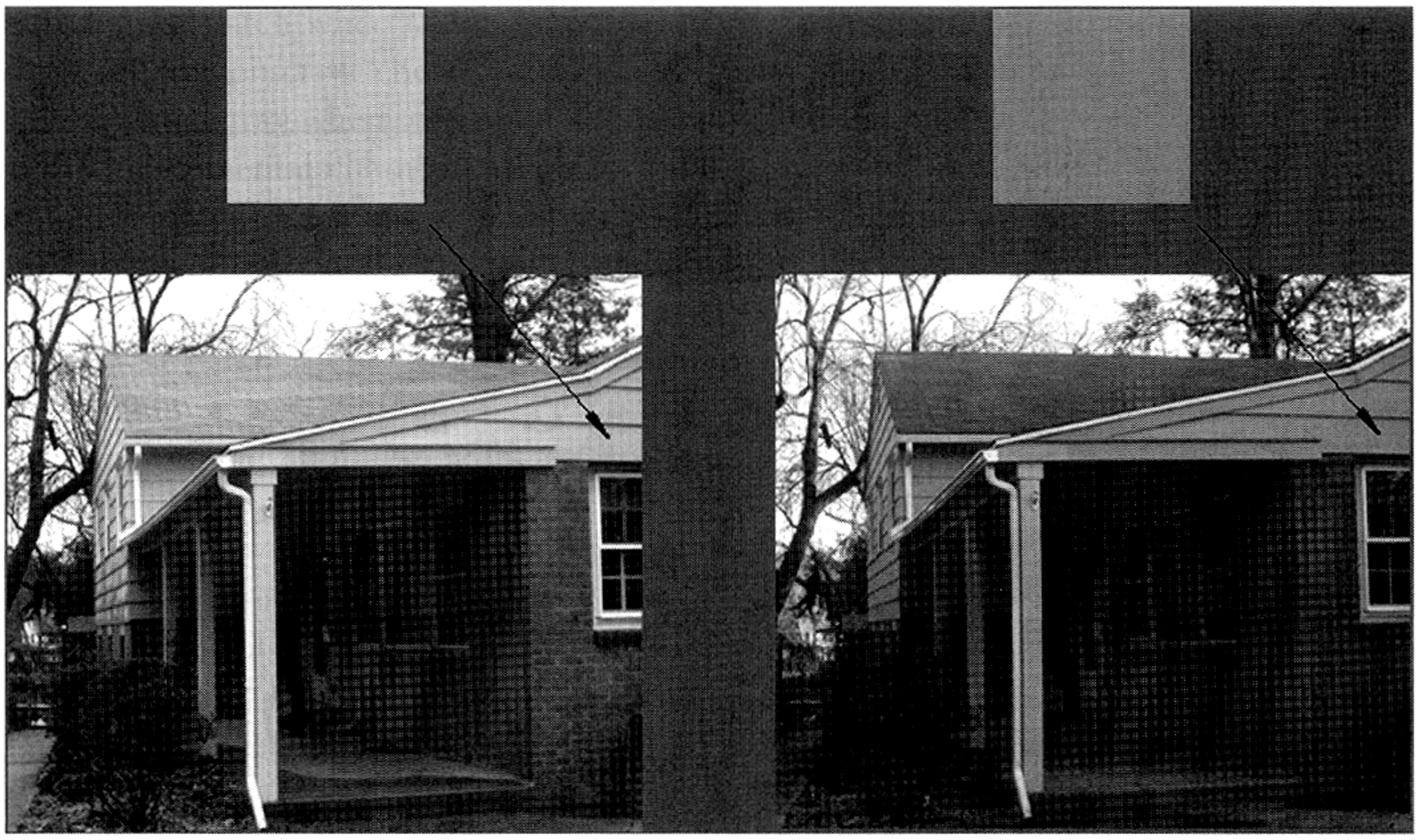

FIGURE 61.1. Same objects imaged under two natural illuminants. *Top*: The patches show a rectangular region extracted from images of the same object under different outdoor illuminants. *Bottom*: The images from which the patches were taken. Images were acquired by the author in Merion Station, Pennsylvania, using a Nikon CoolPix 995 digital camera. The automatic white balancing calculation that is a normal part of the camera's operation was disabled during image acquisition. (See color plate 36.)

experimentally and how it can be understood. The next section presents an extended example of how constancy is measured in the laboratory. The measurements show both circumstances where constancy is good and those where it is not; a characterization of human color vision as either "approximately color constant" or "not very color constant" is too simple. Rather, we must characterize when constancy will be good and when it will not. The discussion outlines two current approaches.

Measuring constancy

This section illustrates how constancy may be measured by describing experiments conducted by Kraft and Brainard (1999; see also Brainard, 1998; Kraft et al., 2002). Before treating the specific experimental design, however, some general remarks are in order.

Several distinct physical processes can cause the illumination impinging on a surface to vary. The images in Figure 61.1 illustrate one such process. They were taken at different times, and the spectra of the illuminant sources changed. Color constancy across illumination changes that occur over time is called *successive color constancy*.

Geometric factors can also cause the illumination impinging on a surface to change. This is illustrated by Figure 61.2. All of the effects shown occur without any change in the spectra of the light sources but instead are induced by the geometry of the light sources and objects. Color constancy across illumination changes that occur within a single scene is called *simultaneous color constancy*.

The visual system's ability to achieve simultaneous constancy need not be easily related to its ability to achieve successive constancy. Indeed, fundamental to simultaneous constancy is some sort of segmentation of the image into regions of common illumination, while such segmentation is not obviously necessary for successive constancy (Adelson, 1999). Often results and experiments about successive and simultaneous constancy are compared and contrasted without explicit acknowledgment that the two may be quite different; keeping the distinction in mind as one considers constancy can reduce confusion. This chapter will focus on successive constancy, as many of the key conceptual issues can be introduced without the extra richness of simultaneous constancy. The discussion returns briefly to simultaneous constancy.

At the beginning of the chapter, constancy was cast in terms of the stability of object color appearance, and this is the sense in which the experiments presented below assess it. Some authors (Brainard and Wandell, 1988; D'Zmura and Mangalick, 1994; Foster and Nascimento, 1994; Khang and Zaidi, 2002) have suggested that constancy might be studied through performance (e.g., object identification) rather than through appearance per se. One might expect appearance to play an important role in identification, but reasoning might also be involved. Although the study of constancy using performance-based methods is an interesting direction, this chapter is restricted to measurements and theories of appearance.

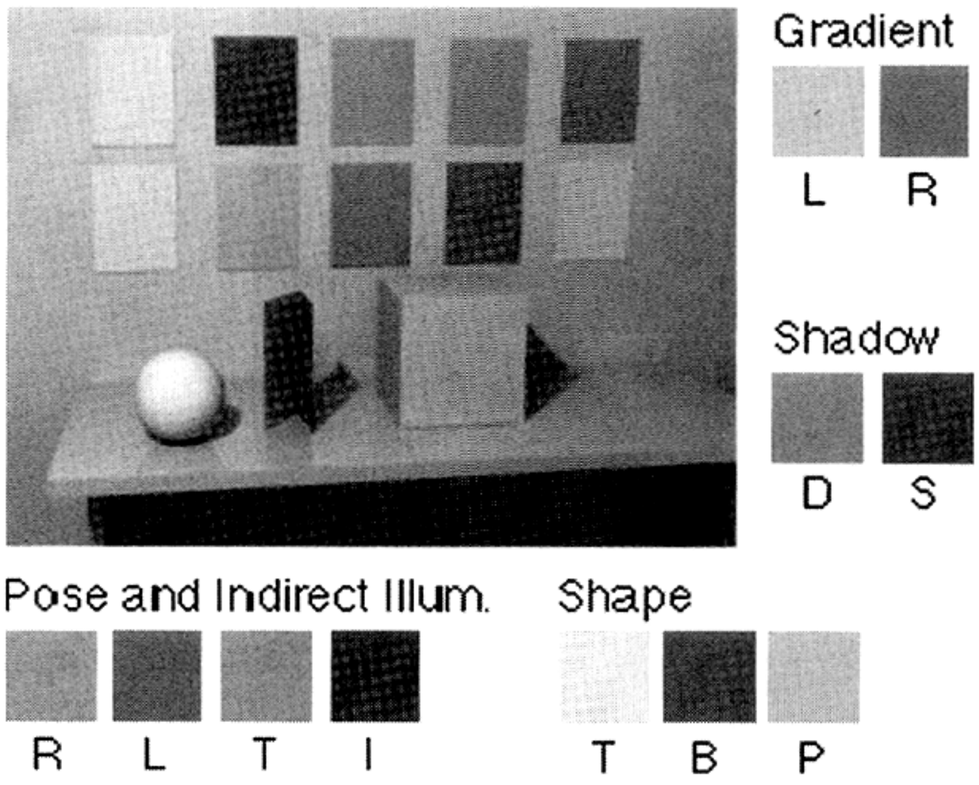

FIGURE 61.2. Image formation. Each set of square patches around the side of the image illustrates variation in the light reflected to the eye when surface reflectance is held fixed. *Gradient*: The two patches shown were extracted from the upper left (L) and lower right (R; above table) of the back wall of the scene. *Shadow*: The two patches were extracted from the tabletop in direct illumination (D) and shadow (S). *Shape*: The three patches shown were extracted from two regions of the sphere (T and B; center top and right bottom, respectively) and from the colored panel directly above the sphere (P; the panel is the leftmost of the four in the bottom row). Both the sphere and the panel have the same simulated surface reflectance function. *Pose and indirect illum*: The four patches were extracted from the three visible sides of the cube (R, L, and T; right, left, and top visible sides, respectively) and from the left side of the folded paper located between the cube and the sphere (I). The simulated surface reflectances of all sides of the cube and of the left side of the folded paper are identical. The image was rendered from a synthetic scene description using the RADIANCE computer graphics package (Larson and Shakespeare, 1998). There were two sources of illumination in the simulated scene: a diffuse illumination that would appear bluish if viewed in isolation and a directional illumination (from the upper left) that would appear yellowish if viewed in isolation. All of the effects illustrated by this rendering are easily observed in natural scenes. (See color plate 37.)

AN EXAMPLE EXPERIMENT Figure 61.3 shows the basic experimental setup used by Kraft and Brainard (1999). Subjects viewed a collection of objects contained in an experimental chamber. The chamber illumination was provided by theater lamps. The light from the lamps passed through a diffuser before entering the chamber, so that the overall effect was of a single diffuse illuminant. Each lamp had either a red, green, or blue filter, and by varying the intensities of the individual lamps, the spectrum of the chamber illumination could be varied. Because the light in the chamber was diffuse, the viewing environment provided a rough approximation to Mondrian World conditions.

The far wall of the experimental chamber contained a *test patch*. Physically, this was a surface of low neutral reflectance so that under typical viewing conditions it would have appeared dark gray. The test patch was illuminated by the

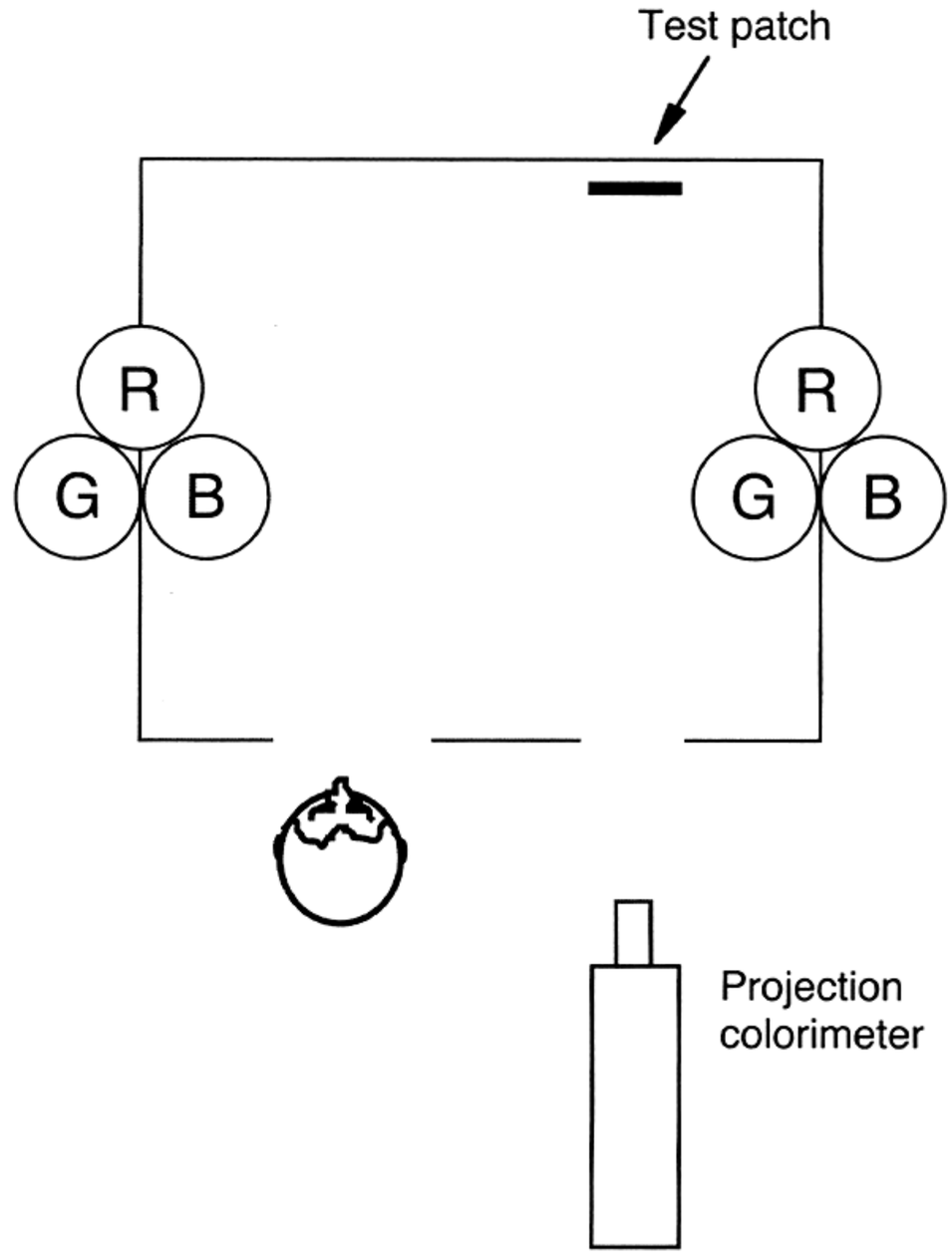

FIGURE 61.3. Schematic diagram of the experimental apparatus used in the experiments of Kraft and Brainard. An experimental chamber was illuminated by computer-controlled theater lamps. Different filters were placed over individual lamps, so that by varying their relative intensity the overall spectral power distribution of the chamber illumination could be varied. The light from the lamps was passed through a diffuser, producing a fairly homogeneous illumination. The observer viewed a test patch on the far wall of the chamber. The test patch was illuminated by the ambient chamber illumination and also by a beam from a projection colorimeter. The beam from the colorimeter was not explicitly visible, so that the perceptual effect of varying it was to change the apparent surface color of the test patch.

ambient chamber illumination and also by a separate projector. The projector beam was precisely aligned with the edges of the test patch and consisted of a mixture of red, green, and blue primaries. By varying the amount of each primary in the mixture, the light reflected to the observer from the test patch could be varied independently of the rest of the image. The effect of changing the projected light was to change the color appearance of the test, as if it had been repainted. The apparatus thus functioned to control the effect described by Gelb (1950; see also Katz, 1935; Koffka, 1935), wherein using a hidden light source to illuminate a paper dramatically changes its color appearance.

The observer's task in Kraft and Brainard's (1999) experiments was to adjust the test patch until it appeared achromatic. Achromatic judgments have been used extensively in the study of color appearance (e.g., Chichilnisky and Wandell, 1996; Helson and Michels, 1948; Werner and Walraven, 1982). During the adjustment, the observer controlled

the chromaticity of the test patch while its luminance was held constant. In essence, the observer chose the test patch chromaticity, which appeared gray when seen in the context set by the rest of the experimental chamber. Whether the test patch appeared light gray or dark gray depended on its luminance. This was held constant during individual adjustments but varied between adjustments. For conditions where the luminance of the test patch is low relative to its surroundings, Brainard (1998) found no dependence of the chromaticity of the achromatic adjustment on test patch luminance. This independence does not hold when more luminous test patches are used (Chichilnisky and Wandell, 1996; Werner and Walraven, 1982).

The data from the experiment are conveniently represented using the standard 1931 CIE chromaticity diagram. Technical explanations of this diagram and its basis in visual performance are widely available (e.g., Brainard, 1995; CIE, 1986; Kaiser and Boynton, 1996), but its key aspects are easily summarized. Human vision is trichromatic, so that a light $C(\lambda)$ may be matched by a mixture of three fixed primaries:

$$C(\lambda) \sim XP_1(\lambda) + YP_2(\lambda) + ZP_3(\lambda) \qquad (2)$$

In this equation $P_1(\lambda)$, $P_2(\lambda)$, and $P_3(\lambda)$ are the spectra of the three primary lights being mixed, and the scalars X, Y, and Z specify the amount of each primary in the mixture. The symbol ~ indicates visual equivalence. When we are concerned with human vision, standardizing a choice of primary spectra allows us to specify a spectrum compactly by its *tristimulus coordinates* X, Y, and Z. The CIE chromaticity diagram is based on a set of known primaries together with a standard of performance that allows computation of the tristimulus coordinates of any light from its spectrum. The chromaticity diagram, however, represents lights with only two coordinates, x and y. These *chromaticity coordinates* are simply normalized versions of the tristimulus coordinates:

$$x = \frac{X}{X+Y+Z}, \quad y = \frac{Y}{X+Y+Z} \qquad (3)$$

The normalization removes from the representation all information about the overall intensity of the spectrum while preserving the information about the relative spectrum that is relevant for human vision.

Figure 61.4 shows data from two experimental conditions. Each condition is defined by the scene within which the test patch was adjusted. The two scenes, labeled Scene 1 and Scene 2, are shown at the top of the figure. The scenes were sparse but had visible three-dimensional structure. The surface lining the chamber was the same in the two scenes, but the spectrum of the illuminant differed. The data plotted for each condition are the chromaticity of the illuminant (*open circles*) and the chromaticity of the observers' achromatic adjustments (*closed circles*).

The points plotted for the illuminant are the chromaticity of the illuminant, as measured at the test patch location when the projection colorimeter was turned off. These represent the chromaticity of the ambient illumination in the chamber, which was approximately uniform. The fact that the illuminant was changed across the two scenes is revealed in the figure by the shift between the open circles.

The plotted achromatic points are the chromaticity of the light reflected to the observer when the test appeared achromatic. This light was physically constructed as the superposition of reflected ambient light and reflected light from the projection colorimeter. Across the two scenes, the chromaticity of the achromatic point shifts in a manner roughly commensurate with the shift in illuminant chromaticity.

RELATION OF THE DATA TO CONSTANCY What do the data plotted in Figure 61.4 say about color constancy across the change from Scene 1 to Scene 2? A natural but misleading intuition is that the large shift in the achromatic locus shown in the figure reveals a large failure of constancy. This would be true if the data plotted represented directly the physical properties of the surface that appears achromatic. As noted above, however, the data plotted describe the spectrum of the light reaching the observer. To relate the data to constancy, it is necessary to combine information from the measured achromatic points and the illuminant chromaticities.

Suppose that the observer perceives the test patch as a surface illuminated with the same ambient illumination as the rest of the chamber. Introspection and some experimental evidence support this assumption (Brainard et al., 1997). The data from Scene 1 can then be used to infer the spectral reflectance of an *equivalent surface*. The equivalent surface would have appeared achromatic had it been placed at the test patch location with the projection colorimeter turned off.

Let the reflectance function of the equivalent surface be $\tilde{S}(\lambda)$. This function must be such that the chromaticity of $E_1(\lambda)\tilde{S}(\lambda)$ is the same as the chromaticity of the measured achromatic point, where $E_1(\lambda)$ is the known spectrum of the ambient illuminant in Scene 1. It is straightforward to find functions $\tilde{S}(\lambda)$ that satisfy this constraint. The inset to Figure 61.4 shows one such function. The function $\tilde{S}(\lambda)$ is referred to as the *equivalent surface reflectance* corresponding to the measured achromatic point.

The equivalent surface reflectance $\tilde{S}(\lambda)$ allows us to predict the performance of a color constant observer for other scenes. To a constant observer, any given surface should appear the same when embedded in any scene. More specifically, a surface that appears achromatic in one scene should remain so in others. Given the data for Scene 1, the chromaticity of the achromatic point for a test patch in Scene 2 should be the chromaticity of $E_2(\lambda)\tilde{S}(\lambda)$, where $E_2(\lambda)$

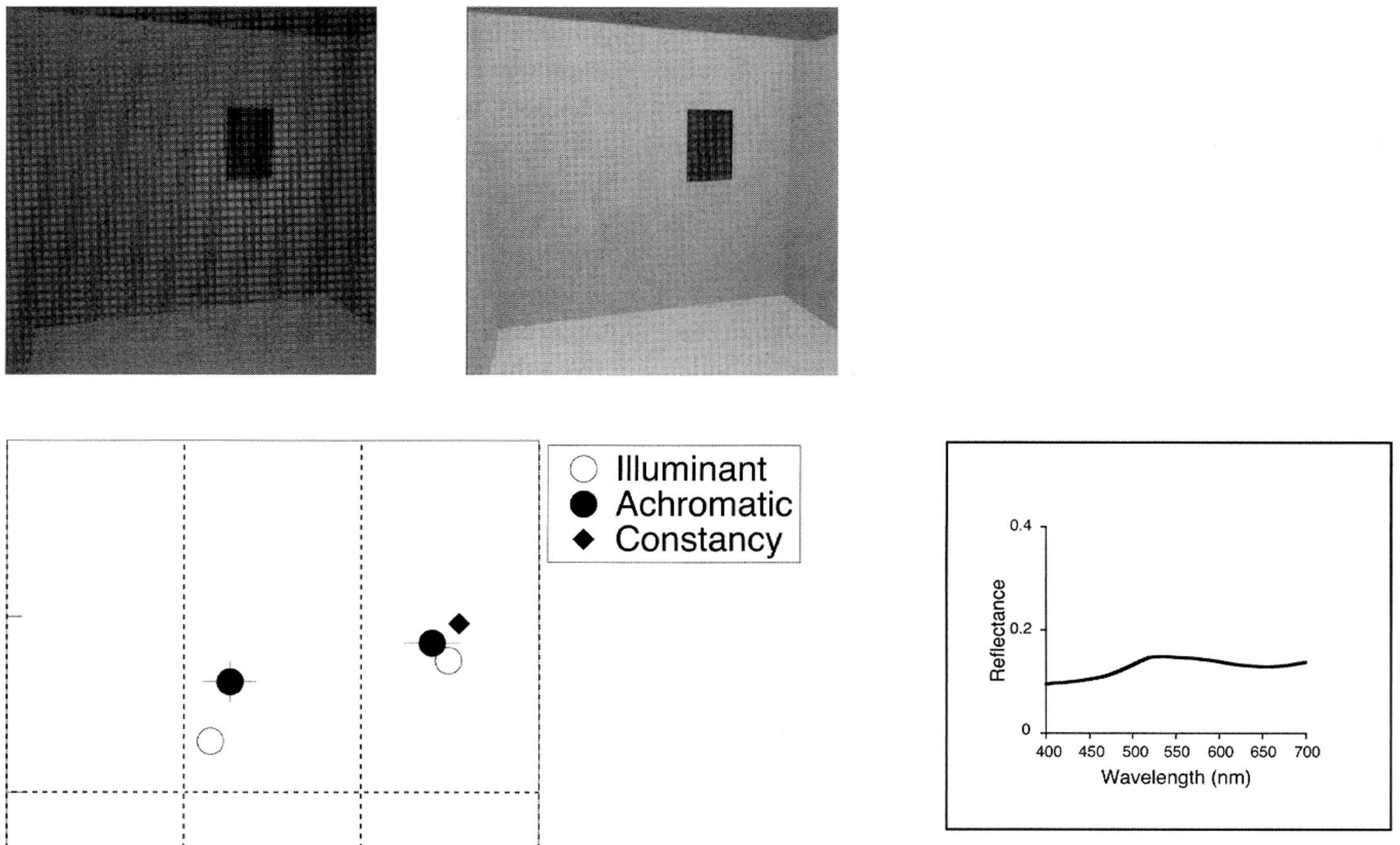

FIGURE 61.4. Basic data from an achromatic adjustment experiment. The images at the top of the figure show the observer's view of two scenes, labeled 1 and 2. The test patch is visible in each image. The projection colorimeter was turned off at the time the images were acquired, so the images do not show the results of observers' achromatic adjustments. The chromaticity diagram shows the data from achromatic adjustments of the test patch made in the context of the two scenes. The open circles show the chromaticity of the illuminant for each scene. The illuminant for Scene 1 plots to the lower left of the illuminant for Scene 2. The closed circles show the chromaticity of the mean achromatic adjustments of four observers. Where visible, the error bars indicate ±1 standard error. The surface reflectance function plotted in the inset at the right of the figure shows the equivalent surface reflectance $\tilde{S}(\lambda)$ computed from the data obtained in Scene 1. The closed diamond shows the color constant prediction for the achromatic adjustment in Scene 2, given the data obtained for Scene 1. See the explanation in the text. (See color plate 38.)

is the spectrum of the illuminant in Scene 2. This prediction is shown in Figure 61.4 by the closed diamond.

Although the measured achromatic point for Scene 2 does not agree precisely with the constancy prediction, the deviation is small compared to the deviation that would be measured for an observer who had no constancy whatsoever. For such an observer, the achromatic point would be invariant across changes of scene. Thus, the data shown in Figure 61.4 indicate that observers are approximately color constant across the two scenes studied in the experiment.

Brainard (1998) developed a constancy index that quantifies the degree of constancy revealed by data of the sort presented in Figure 61.4. The index takes on a value of 0 for no adjustment and 1 for perfect constancy, with intermediate values for intermediate performance. For the data shown in Figure 61.4, the constancy index is 0.83. This high value seems consistent with our everyday experience that the colors of objects remain stable over changes of illuminant but that the stability is not perfect.

A PARADOX AND ITS RESOLUTION The introductory section stated that illuminant and surface information is perfectly confounded in the retinal image. The data shown in Figure 61.4 indicate that human vision can separate

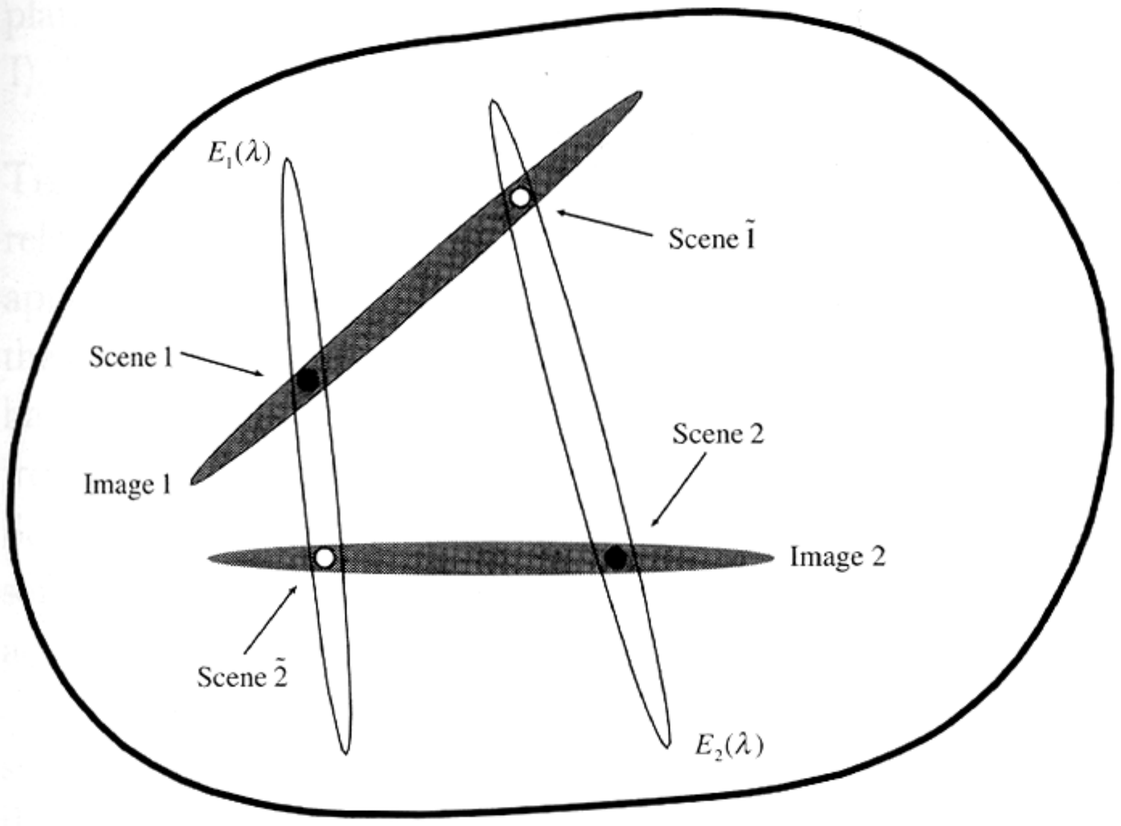

FIGURE 61.5. Schematic illustration of the ambiguity inherent in color constancy. The figure shows schematically the set of all scenes. Each point in the schematic represents a possible scene. Scenes 1 and 2 from the experiment described in text are indicated by closed circles. Each shaded ellipse encloses a subset of scenes that all produce the same image. The scenes represented by open circles, Scenes $\tilde{1}$ and $\tilde{2}$, produce the same images as Scenes 1 and 2, respectively. The open ellipses each enclose a subset of scenes that share the same illuminant.

these confounded physical factors and achieve approximate color constancy. This presents a paradox. If the information is perfectly confounded, constancy is impossible. If constancy is impossible, how can the visual system be achieving it?

The resolution to this paradox is found by considering restrictions on the set of scenes over which constancy holds. Figure 61.5 shows a schematic diagram of the set of all scenes, represented by the thick outer boundary. Each point within this boundary represents a possible scene, that is, a particular choice of illuminant and surface reflectances. The closed circles represent the two scenes used in the experiment described above. These are labeled Scene 1 and Scene 2 in the figure.

Denote the retinal image produced from Scene 1 as Image 1. Many other scenes could have produced this same image. This subset of scenes is indicated in the figure by the shaded ellipse that encloses Scene 1. This ellipse is labeled Image 1 in the figure. It also contains Scene $\tilde{1}$, indicated by an open circle in the figure. Scenes 1 and $\tilde{1}$ produce the same image and cannot be distinguished by the visual system.

Similarly, there is a separate subset of scenes that produce the same image (denoted Image 2) as Scene 2. This subset is also indicated by a shaded ellipse. A particular scene consistent with Image 2 is indicated by the open circle labeled Scene $\tilde{2}$. Like Scenes 1 and $\tilde{1}$, Scenes 2 and $\tilde{2}$ cannot be distinguished from each other by the visual system.

The open ellipse enclosing each solid circle shows a different subset of scenes to which it belongs. These are scenes that share a common illuminant. The open ellipse enclosing Scene 1 indicates all scenes illuminated by $E_1(\lambda)$, while the open ellipse enclosing Scene 2 indicates all scenes illuminated by $E_2(\lambda)$.

The figure illustrates why constancy is impossible in general. When viewing Image 1, the visual system cannot tell whether Scene 1 or Scene $\tilde{1}$ is actually present: achromatic points measured for a test patch embedded in these two scenes must be the same, even though the scene illuminants are as different as they are for Scenes 1 and 2. Recall from the data analysis above that this result (no change of achromatic point across a change of illuminant) indicates the absence of constancy.

The figure also illustrates why constancy can be shown across some scene pairs. Scenes 1 and 2 produce distinguishable retinal images, so there is no a priori reason for the measured achromatic points for test patches embedded in these two scenes to bear any relation to each other. In particular, there is no constraint that prevents the change in achromatic points across the two scenes from tracking the corresponding illuminant change. Indeed, one interpretation of the good constancy shown by the data reported above is that the visual system infers approximately the correct illuminants for Scenes 1 and 2. A mystery would occur only if it could also infer the correct illuminants for Scenes $\tilde{1}$ and $\tilde{2}$.

Figure 61.6 replots the results from achromatic measurements made for Scene 1 together with the results for a new scene, $\tilde{1}$. The illuminant in Scene $\tilde{1}$ is the same as that in Scene 2, but the objects in the scene have been changed to make the image reflected to the eye for Scene $\tilde{1}$ highly similar to that reflected for Scene 1; Scene $\tilde{1}$ is an experimental approximation to the idealized Scene $\tilde{1}$ described above. It would be surprising indeed if constancy were good when assessed between Scenes 1 and $\tilde{1}$, and it is not. The achromatic points measured for Scenes 1 and $\tilde{1}$ are very similar, with the constancy index between them being 0.11.

Discussion

CONSTANCY DEPENDS ON THE IMAGE ENSEMBLE STUDIED

The analysis and data presented above show that the degree of human color constancy depends on the choice of scenes across which it is assessed. Thus, it is not useful to summarize human performance through blanket statements about the degree of constancy obtained. Rather, questions about constancy must be framed in conjunction with a specification of the scene ensemble. Natural questions are (1) what ensembles of scenes support good constancy? and (2) how does constancy vary within some ensemble of scenes which

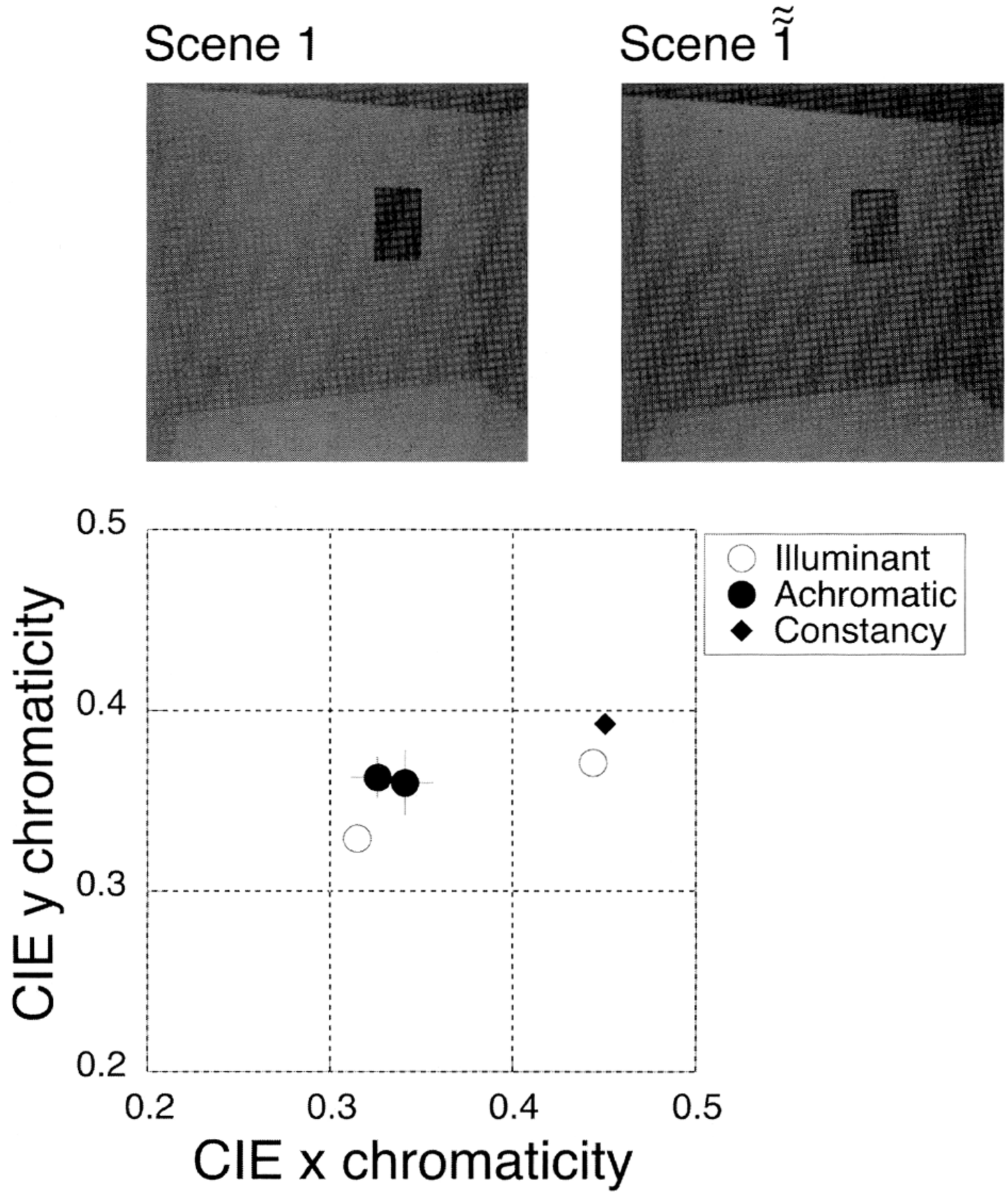

FIGURE 61.6. Achromatic data when both illuminant and scene surfaces are varied. The images at the top of the figure show the observer's view of two scenes, labeled 1 and $\tilde{1}$. The relation between these scenes is described in the text. The test patch is visible in each image. The projection colorimeter was turned off at the time the images were acquired, so the images do not show the results of observers' achromatic adjustments. The chromaticity diagram shows the data from achromatic adjustments of the test patch made in the context of the two scenes. The format is the same as that of Figure 61.4. The equivalent surface reflectance $\tilde{S}(\lambda)$ computed from the data obtained in Scene 1 is shown in Figure 61.4. (See color plate 39.)

is intrinsically of interest? An example of the latter would be scenes that occur in natural viewing.

The choice of experimental scenes is a crucial aspect of the design of any constancy experiment. Without some a priori restriction the number of possible scenes is astronomical, and systematic exploration of the effect of all possible stimulus variables is not feasible. In choosing an ensemble of scenes for study, different experimenters have been guided by different intuitions. Indeed, it is this choice that most differentiates various studies. A common rationale, however, is to test specific hypotheses about how constancy might operate. The goal is to develop principles that allow generalization beyond the scenes studied experimentally.

Two broad approaches have been pursued. The *mechanistic approach* is based on the hope that constancy is mediated by simple visual mechanisms and that these mechanisms can be studied through experiments with simple stimuli (e.g., uniform test patches presented on uniform background fields). The *computational approach* is to develop image processing algorithms that can achieve color constancy and to use insight gained from the algorithms to build models of human performance. This approach is often characterized by the use of stimuli closer to those encountered in natural viewing, as the algorithms are generally designed to take advantage of the statistical structure of natural images. The difference between the mechanistic and computational approaches is not always clear-cut: a mechanistic theory that explains human constancy can always be recast as a computational algorithm, while the action of a given algorithm can probably be approximated by the action of a series of

plausible neural mechanisms (see, e.g., Marr, 1982, chapter 1). Examples of both approaches are outlined below.

THE MECHANISTIC APPROACH Constancy is essentially a relative phenomenon; it can be assessed only by measuring appearance across two (or more) scenes. We cannot say from the data above that constancy is good for Scenes 1 and 2 but bad for Scene $\tilde{1}$. Rather, constancy is good across the change from Scene 1 to Scene 2 but bad across the change from Scene 1 to Scene $\tilde{1}$. Presumably it is possible to construct some other Scene 3 such that good constancy is revealed across Scenes $\tilde{1}$ and 3.

What is it about the relation between Scenes 1 and 2 that supports the good constancy observed? A critical feature is that all that differs between them is the spectrum of the ambient illuminant. This design is common to most studies of constancy—stability of appearance is assessed under conditions where the surfaces comprising the scene are held fixed while the illuminant is varied (e.g., Arend and Reeves, 1986; Brainard and Wandell, 1992; Breneman, 1987; Burnham et al., 1957; Helson and Jeffers, 1940; McCann et al., 1976). It is probably the ubiquity of this surfaces-held-fixed design that leads to the oft-quoted generalization that human vision is approximately color constant (e.g., Boring, 1942).

When the surfaces in the image are held constant, it is easy to postulate mechanisms that could, qualitatively at least, support the high levels of observed constancy.

The initial encoding of the color signal by the visual system is the absorption of light quanta by photopigment in three classes of cone photoreceptors, the L, M, and S cones (for a fuller treatment see, e.g., Brainard, 1995; Kaiser and Boynton, 1996; Rodieck, 1998). The three classes are distinguished by how their photopigments absorb light as a function of wavelength. The fact that color vision is based on absorptions in three classes of cones is the biological substrate for trichromacy.

An alternative to using tristimulus or chromaticity coordinates to represent spectral properties of the light reaching the eye is to use cone excitation coordinates. These are proportional to the quantal absorption rates for the three classes of cones elicited by the light. The cone excitation coordinates for a light, $\mathbf{r}$, may be specified by using a three-dimensional column vector

$$\mathbf{r} = \begin{bmatrix} r_L \\ r_M \\ r_S \end{bmatrix} \tag{4}$$

It is well accepted that the signals initiated by quantal absorption are regulated by adaptation. A first-order model of adaptation postulates that (1) the adapted signals are determined from quantal absorption rates through multiplicative gain control; (2) at each retinal location the gains are set independently within each cone class, so that (e.g.,) signals from M and S cones do not influence the gain of L cones; and (3) for each cone class, the gains are set in inverse proportion to a spatial average of the quantal absorption rates seen by cones of the same class. This model is generally attributed to von Kries (1905/1970). The three postulates together are sometimes referred to as *von Kries adaptation.* Von Kries recognized that models where some of the postulates hold and others do not could also be considered.

The first postulate of von Kries adaptation asserts that for each cone class, there is an adapted cone signal (a_L for the L cones, a_M for the M cones, and a_S for the S cones) that is obtained from the corresponding cone excitation coordinate through multiplication by a gain (e.g., $a_L = g_L r_L$). This may be expressed using the vector notation introduced in Eq. (4). Let the vector $\mathbf{a}$ represent the magnitude of the adapted cone signals. Then

$$\mathbf{a} = \begin{bmatrix} a_L \\ a_M \\ a_S \end{bmatrix} = \begin{bmatrix} g_L & 0 & 0 \\ 0 & g_M & 0 \\ 0 & 0 & g_S \end{bmatrix} \begin{bmatrix} r_L \\ r_M \\ r_S \end{bmatrix} = \mathbf{D}\mathbf{r} \tag{5}$$

Because the adapted cone signals $\mathbf{a}$ are obtained from the cone excitation coordinates $\mathbf{r}$ through multiplication by the diagonal matrix $\mathbf{D}$, this postulate is called the *diagonal model for adaptation.* It should be emphasized that for the diagonal model to have predictive power, *all* of the effect of context on color processing should be captured by Eq. (5). In this model, two test patches that have the same adapted cone signals should have the same appearance.

In general, it is conceptually useful to separate two components of a model of adaptation (Brainard and Wandell, 1992; Krantz, 1968). The first component specifies what parameters of a visual processing model are allowed to vary with adaptation. The diagonal model provides this component of the full von Kries model. In the diagonal model, the only parameters that can vary are the three gains.

The second component of a full model specifies how the processing parameters are determined by the image. The diagonal model is silent about this, but the issue is addressed by the second two assumptions of the full von Kries model. Only cone excitation coordinates within a cone class influence the gain for that cone class, and the specific form of the influence is that the gain at a location is set inversely proportional to the mean excitation in a neighborhood of the location.

If the visual system implements von Kries adaptation, the adapted cone signals coding the light reflected from a surface are considerably stabilized across illuminant variation, provided that the other surfaces in the scene also remain fixed (Brainard and Wandell, 1986; Foster and Nascimento, 1994; Lennie and D'Zmura, 1988; see also Finlayson et al., 1994). Indeed, von Kries adaptation is the active ingredient

in later versions of Land's popular *retinex* account of successive color constancy. In the descriptions of the retinex algorithm, the adapted cone signals are called *lightness designators*, and these are derived from cone excitations through elaborate calculation. Nonetheless, for successive constancy the calculation reduces to a close approximation to classic von Kries adaptation (Land, 1986; see Brainard and Wandell, 1986; for early descriptions of Land's work see Land, 1959a, 1959b; Land and McCann, 1971).

Qualitatively, then, von Kries adaptation can explain the good constancy shown in experiments where the illuminant is changed and the surfaces in the scene are held fixed. Such adaptation also provides a qualitative account for the poor constancy shown by the data in Figure 61.6, where both the illuminant and surfaces in the scene were changed to hold the image approximately constant. On the basis of the data presented so far, one might sensibly entertain the notion that human color constancy is a consequence of early adaptive gain control.

Each of the postulates of von Kries adaptation have been subjected to sharply focused empirical test, and it is clear that each fails when examined closely. With respect to the diagonal model, a number of experimental results suggest that there must be additional adaptation that is not described by Eq. (5). These effects include gain control at neural sites located after signals from different cone classes combine and signal regulation characterized by a subtractive process rather than multiplicative gain control (e.g., Hurvich and Jameson, 1958; Jameson and Hurvich, 1964; Poirson and Wandell, 1993; Shevell, 1978; Walraven, 1976; see also Eskew et al., 1999; Webster, 1996).

The diagonal model fails when probed with stimuli carefully crafted to test its assumptions. Does it also fail for natural scenes? The illuminant spectral power distributions $E(\lambda)$ and surface spectral reflectance functions $S(\lambda)$ found in natural scenes are not arbitrary. Rather, these functions tend to vary smoothly as a function of wavelength. This constraint restricts the range of color signals likely to occur in natural scenes. Conditions that elicit performance in contradiction to the diagonal model may not occur for natural scenes. If so, the diagonal model would remain a good choice for studies of how adaptive parameters vary within this restricted domain.

The regularity of illuminant and surface spectral functions may be captured with the use of small-dimensional linear models (e.g., Cohen, 1964; Jaaskelainen et al., 1990; Judd et al., 1964; Maloney, 1986). The idea of a linear model is simple. The model is defined by N basis functions. These are fixed functions of wavelength, $E_1(\lambda), \ldots, E_N(\lambda)$. Any spectrum $E(\lambda)$ is approximated within the linear model by a weighted sum of the basis functions

$$\tilde{E}(\lambda) = w_1 E_1(\lambda) + \ldots + w_N E_N(\lambda) \qquad (6)$$

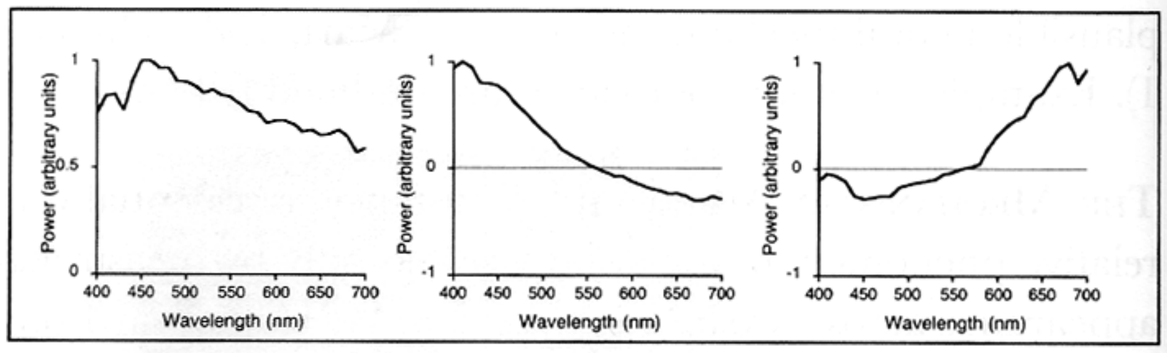

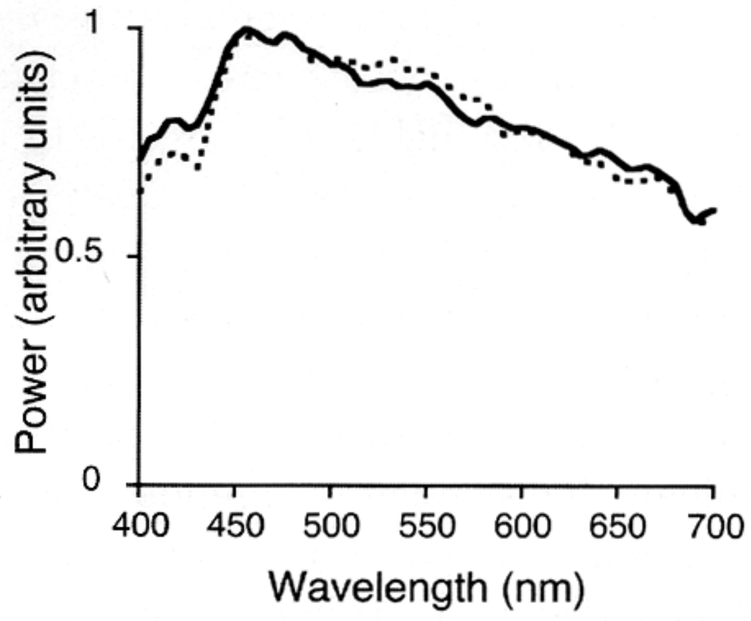

FIGURE 61.7. Linear model for natural daylights. *Top*: Three basis functions for the CIE linear model for daylights (CIE, 1986). *Bottom*: Linear model approximation to measured daylight. Solid line, measurement. Dotted line, reconstruction. The measured daylight was obtained from a database of measurements made available by J. Parkkinen and P. Silfsten on the World Wide Web at http://cs.joensuu.fi/~spectral/databases/download/daylight.htm.

where the weights are chosen to minimize the approximation error. Figure 61.7 plots the basis functions of a three-dimensional linear model for natural daylight and shows the linear model approximation to a measured daylight. The same approach can be used to express constraints on surface reflectance functions. The use of linear models has been central to computational work on color constancy (Brainard and Freeman, 1997; Brainard et al., in press; Maloney, 1999).

Mondrian World scenes where the illuminants and surface spectra are restricted to be typical of naturally occurring spectra can be referred to as *Restricted Mondrian World* scenes. When the experimental scenes are from the Restricted Mondrian World, the diagonal model seems to provide a good description of performance.

Brainard and Wandell (1992) tested the diagonal model using *asymmetric matching*. In asymmetric matching, the observer adjusts a matching patch, embedded in one scene, so that its appearance matches that of a test patch presented in another. In the context of the diagonal model, the match is taken to indicate two lights that elicit identical adapted cone signals. Let $\mathbf{a}^t$ and $\mathbf{a}^m$ represent the adapted cone signals for the test and matching patches. Equation (5) then yields

$$\mathbf{a}^t = \mathbf{D}^t\mathbf{r}^t = \mathbf{a}^m = \mathbf{D}^m\mathbf{r}^m \Rightarrow \mathbf{r}^m = [\mathbf{D}^m]^{-1}[\mathbf{D}^t]\mathbf{r}^t = \mathbf{D}^{t\to m}\mathbf{r}^t \qquad (7)$$

where the diagonal matrix $\mathbf{D}^{t\to m}$ is

$$\mathbf{D}^{t\to m} = \begin{bmatrix} \frac{g_L^t}{g_L^m} & 0 & 0 \\ 0 & \frac{g_M^t}{g_M^m} & 0 \\ 0 & 0 & \frac{g_S^t}{g_S^m} \end{bmatrix} \tag{8}$$

If the diagonal model is correct, the cone excitation coordinates of the test and match patches are related by a diagonal matrix whose entries are the ratios of cone gains. A single asymmetric match determines the entries of the matrix $\mathbf{D}^{t\to m}$. Since Eq. (7) must hold with the same matrix $\mathbf{D}^{t\to m}$ for any choice of test patch cone coordinates, repeating the experiment with different test patches allows evaluation of the diagonal model.

In a successive matching experiment that employed simple synthetic scenes, Brainard and Wandell (1992) found that a large set of asymmetric matching data was in good agreement with the diagonal model. Similar results were obtained by Bauml (1995) also for successive matching and by Brainard et al. (1997) for simultaneous matching. To develop a theory of color constancy that applies to natural viewing, violations of the diagonal model may be small enough to neglect.

What about the other postulates of von Kries adaptation, which concern how the gains are set by image context? The notion that the gains are set as a function of a spatial average of the image has been tested in a number of ways. One approach is to examine the *equivalent background hypothesis*. In its general form, this hypothesis asserts that the effect of any image on the color appearance of a test light is the same as that of some uniform background. If the gains are set by a spatial average of the image, then the equivalent background hypothesis must also hold.

Precise tests of the equivalent background hypothesis where spatial variation of color is introduced into a uniform background, indicate that it fails (Brown and MacLeod, 1997; Shevell and Wei, 1998). The general logic is first to find a uniform field and a spatially variegated field that have an identical effect on the appearance of a single test light and then show that for some other test light these two contexts have different effects (Stiles and Crawford, 1932). Like the sharpest tests of the diagonal model, however, these studies did not employ stimuli from the Restricted Mondrian World.

Kraft and Brainard (1999) examined whether the spatial mean of an image controls the state of adaptation by constructing two illuminated scenes that had the same spatial mean. To equate the mean, both the illuminant and the scene surfaces were varied between the scenes. Kraft and Brainard then measured the achromatic loci in the two scenes. If the spatial mean were the only factor controlling adaptation, then the achromatic point in the two scenes should have been the same. A more general constancy mechanism, however, might be able to detect the change in the illuminant based on some other aspect of the images. The achromatic points were distinct, with a mean constancy index of 0.39. Even for nearly natural scenes, control of the gains is not a simple function of the spatial mean of the image: the visual system has access to additional cues to the illuminant. Kraft and Brainard examined other simple hypotheses about control of adaptation in nearly natural scenes and found that none accounted for the data.

A key feature in Kraft and Brainard's (1999) design (see also Gilchrist and Jacobson, 1984; Kraft et al., 2002; McCann, 1994) is that both the illuminant and the surfaces in the scene were varied. When only the illuminant is varied, the data are roughly consistent with adaptation to the spatial mean of the image. Such data do not provide a sharp test, however, since essentially all plausible hypotheses predict good constancy when the surfaces in the image are held fixed across an illuminant change. Only by varying the surfaces and illuminants to differentiate predictions can strong tests be made. This point also applies to studies of the neural locus of constancy.

The current state of affairs for the mechanistic approach may be summarized roughly as follows. A gain control model provides a reasonable approximation to performance measured in scenes consisting of illuminated surfaces, but lacking is a theory that links the gains to the image. The agenda is to understand what image factors control the state of adaptation. In the lightness literature, this is sometimes referred to as the *anchoring problem* (e.g., Gilchrist et al., 1999). Within the mechanistic approach, one recent theme is to study the influence of image contrast (Brown and MacLeod, 1997; Golz and MacLeod, 2002; Krauskopf et al., 1982; Shevell and Wei, 1998; Singer and D'Zmura, 1995; Webster and Mollon, 1991) and spatial frequency content (Bauml and Wandell, 1996; Poirson and Wandell, 1993). Another approach (Bauml, 1995; Brainard and Wandell, 1992; Chichilnisky and Wandell, 1995) is to study rules of combination (e.g., linearity) that allow prediction of parameter values for many images on the basis of measurements made for just a few.

THE COMPUTATIONAL APPROACH The mechanistic approach is motivated by consideration of the physiology and anatomy of the visual pathways. The computational approach begins with consideration about how one could, in principle, process the retinal image to produce a stable representation of surface color. The computational approach focuses on the information contained in the image rather than on the specific operation of mechanisms that extract the information.

Computational algorithms often operate in two distinct steps (Maloney, 1999). The first step estimates the illuminant

at each image location, while the second step uses the estimate to transform the cone coordinates at each location to an illuminant-invariant representation. Given linear model constraints on natural surface reflectance functions, the second step is quite straightforward (Buchsbaum, 1980) and is well approximated by diagonal gain control (Brainard and Wandell, 1986; Foster and Nascimento, 1994). The deep issue is what aspects of the image carry useful information about the illuminant. This issue is completely analogous to the central issue within the mechanistic approach, namely, what aspects of the image control adaptation. Indeed, the idea linking the computational algorithms to measured human performance is that measured adaptation might be governed by the same image statistics that provide information about the illuminant (Brainard et al., in press; Maloney, 1999).

Many algorithms have been proposed for estimating the illuminant from the image (Brainard and Freeman, 1997; Buchsbaum, 1980; D'Zmura and Iverson, 1993; D'Zmura et al., 1995; Finlayson et al., 1997; Forsyth, 1990; Funt and Drew, 1988; Lee, 1986; Maloney and Wandell, 1986). A detailed review of the individual algorithms is beyond the scope of this chapter, but excellent reviews are available (Hurlbert, 1998; Maloney, 1999). Common across algorithms is the general approach of specifying assumptions that restrict the class of scenes and then showing how it is possible to estimate the illuminant within the restricted class. With reference to Figure 61.5, each algorithm is based on a rule for choosing one particular scene from within each shaded ellipse.

In practice, different proposed algorithms depend on different image statistics. For example, in Buchsbaum's (1980) classic algorithm, the illuminant estimate was based on the spatial mean of the cone quantal absorption rates. As a model for human performance, this algorithm may be tested by asking whether adaptation is governed only by the spatial mean. As described above, experiments show that this is not the case. The detailed logic connecting this algorithm to human performance is described in a recent review (Brainard et al., in press).

Other computational algorithms depend on different aspects of the image. For example, Lee (1986; see also D'Zmura and Lennie, 1986) showed that specular highlights in an image carry information about the illuminant. This has led to tests of whether human vision takes advantage of the information contained in specular highlights (Hurlbert et al., 1989; Yang and Maloney, 2001).

In Yang and Maloney's (2001) work, the stimuli consisted of realistic computer graphics renderings of synthetic scenes. That is, the locations, spectral properties, and geometric properties of the scene illuminants and surfaces were specified in software, and a physics-based rendering algorithm was used to generate the stimuli. In real scenes, the information provided by separate cues tends to covary, which makes it difficult to separate their effects. By using synthetic imagery, Yang and Maloney teased apart the effects of independent cues. They were able to show that specular highlights can influence human judgments of surface color appearance and to begin to delineate the circumstances under which this happens. Delahunt (2001) employed similar techniques to study the role of prior information about natural daylights in successive color constancy. (For computational analysis of the use of such prior information, see Brainard and Freeman, 1997; D'Zmura et al., 1995). The methodology promises to allow systematic study of a variety of hypotheses extracted from the computational literature.

GENERALIZING TO SIMULTANEOUS CONSTANCY This chapter has focused on successive color constancy, and in particular on the case where the illuminant is approximately uniform across the scene. As illustrated by Figure 61.2, this idealized situation does not hold for natural scenes.

When an image arises from a scene with multiple illuminants, one can still consider the problem of successive color constancy. That is, one can ask what happens to the color appearance of an object in the scene when the spectral properties of the illuminant are changed without a change in scene geometry. Little, if any, experimental effort has been devoted to this question.

The case of spatially rich illumination also raises the question of simultaneous constancy—how similar does the same object appear when located at different places within the scene?

One thread of the literature has emphasized the role of scene geometry (Bloj and Hurlbert, 2002; Bloj et al., 1999; Epstein, 1961; Flock and Freedberg, 1970; Gilchrist, 1977, 1980; Hochberg and Beck, 1954; Knill and Kersten, 1991; Pessoa et al., 1996). Under some conditions, the perceived orientation of a surface in a scene can influence its apparent lightness and color in a manner that promotes constancy. The range of conditions under which this happens, however, is not currently well understood.

An interesting aspect of simultaneous constancy is that the observer's performance can depend heavily on experimental instructions. In a study of simultaneous color constancy, Arend and Reeves (1986) had observers adjust the color of one region of a stimulus display until it appeared the same as another. They found that observers' matches varied with whether they were asked to judge the color of the reflected light or the color of the underlying surface. More constancy was shown when observers were asked to judge the surface (see also Bauml, 1999; Bloj and Hurlbert, 2002). In a study of successive constancy, on the other hand, Delahunt (2001) found only a small instructional effect. It is not yet clear what conditions support the instructional dichotomy, or whether

the dichotomy indicates dual perceptual representations or observers' ability to reason from appearance to identity.

Recent theories of lightness perception have emphasized simultaneous constancy (Adelson, 1999; Gilchrist et al., 1999). At the core of these theories is that idea that perception of lightness (and presumably color) proceeds in two basic stages. First, the visual system segments the scene into separate regions. Second, image data within regions are used to set the state of adaptation for that region. (At a more detailed level, the theories also allow for some interaction between the states of adaptation in different regions.) The two-stage conception provides one way that results for successive constancy might generalize to handle simultaneous constancy: models that explain successive constancy for uniformly illuminated scenes might also describe the processes that set the state of adaptation within separately segmented regions within a single image (Adelson, 1999). To the extent that this hypothesis holds, it suggests that work on simultaneous constancy should focus on the segmentation process. At the same time, it must be recognized that the segment-estimate hypothesis is not the only computational alternative (see, e.g., Adelson and Pentland, 1996; Funt and Drew, 1988; Land and McCann, 1971; Zaidi, 1998) and that empirical tests of the general idea should also be given high priority.

Acknowledgments

I thank P. Delahunt, B. Wandell, and J. Werner for discussion and for comments on draft versions of this chapter. This work was supported by National Eye Institute Grant EY 10016.

REFERENCES

Adelson, E. H., 1999. Lightness perception and lightness illusions, in *The New Cognitive Neurosciences*, 2nd ed. (M. Gazzaniga ed.), Cambridge, MA: MIT Press, pp. 339–351.

Adelson, E. H., and A. P. Pentland, 1996. The perception of shading and reflectance, in *Visual Perception: Computation and Psychophysics* (D. Knill and W. Richards, eds.), New York: Cambridge University Press, pp. 409–423.

Arend, L. E., and A. Reeves, 1986. Simultaneous color constancy, *J. Opt. Soc. Am. A*, 3:1743–1751.

Bauml, K. H., 1995. Illuminant changes under different surface collections: examining some principles of color appearance, *J. Opt. Soc. Am. A*, 12:261–271.

Bauml, K. H., 1999. Simultaneous color constancy: how surface color perception varies with the illuminant, *Vis. Res.*, 39:1531–1550.

Bauml, K. H., and B. A. Wandell, 1996. Color appearance of mixture gratings, *Vis. Res.*, 36:2849–2864.

Bloj, M. G., and A. C. Hurlbert, 2002. An empirical study of the traditional Mach card effect, *Perception*, 31:233–246.

Bloj, M., D. Kersten, and A. C. Hurlbert, 1999. Perception of three-dimensional shape influences colour perception through mutual illumination, *Nature*, 402:877–879.

Boring, E. G., 1942. *Sensation and Perception in the History of Experimental Psychology*, New York: D. Appleton Century.

Brainard, D. H., 1995. Colorimetry, in *Handbook of Optics*, vol. 1, *Fundamentals, Techniques, and Design* (M. Bass ed.), New York: McGraw-Hill, pp. 26.1–26.54.

Brainard, D. H., 1998. Color constancy in the nearly natural image. 2. Achromatic loci, *J. Opt. Soc. Am. A*, 15:307–325.

Brainard, D. H., W. A. Brunt, and J. M. Speigle, 1997. Color constancy in the nearly natural image. 1. Asymmetric matches, *J. Opt. Soc. Am. A*, 14:2091–2110.

Brainard, D. H., and W. T. Freeman, 1997. Bayesian color constancy, *J. Opt. Soc. Am. A*, 14:1393–1411.

Brainard, D. H., J. M. Kraft, and P. Longère (in press). Color constancy: developing empirical tests of computational models, in *Colour Perception: From Light to Object* (R. Mausfeld and D. Heyer, eds.), Oxford: Oxford University Press.

Brainard, D. H., and B. A. Wandell, 1986. Analysis of the retinex theory of color vision, *J. Opt. Soc. Am. A*, 3:1651–1661.

Brainard, D. H., and B. A. Wandell, 1988. Classification measurement of color appearance, *Invest. Opthalmol. Vis. Sci., Suppl.*, 29:162.

Brainard, D. H., and B. A. Wandell, 1992. Asymmetric color-matching: how color appearance depends on the illuminant, *J. Opt. Soc. Am. A*, 9:1433–1448.

Breneman, E. J., 1987. Corresponding chromaticities for different states of adaptation to complex visual fields, *J. Opt. Soc. Am. A*, 4:1115–1129.

Brown, R. O., and D. I. A. MacLeod, 1997. Color appearance depends on the variance of surround colors, *Curr Biol.*, 7:844–849.

Buchsbaum, G., 1980. A spatial processor model for object colour perception, *J. Franklin Inst.*, 310:1–26.

Burnham, R. W., R. M. Evans, and S. M. Newhall, 1957. Prediction of color appearance with different adaptation illuminations, *J. Opt. Soc. Am.*, 47:35–42.

Chichilnisky, E. J., and B. A. Wandell, 1995. Photoreceptor sensitivity changes explain color appearance shifts induced by large uniform backgrounds in dichoptic matching, *Vis. Res.*, 35:239–254.

Chichilnisky, E. J., and B. A. Wandell, 1996. Seeing gray through the on and off pathways, *Vis. Neurosci.*, 13:591–596.

CIE, 1986. *Colorimetry*, 2nd ed. (CIE Pub. 15.2), Vienna, Bureau Central de la CIE.

Cohen, J., 1964. Dependency of the spectral reflectance curves of the Munsell color chips, *Psychon. Sci.*, 1:369–370.

Delahunt, P. B., 2001. *An evaluation of color constancy across illumination and mutual reflection changes.* Unpublished Ph.D. thesis, Uniueisity of California at Santa Barbara, Santa Barbara.

D'Zmura, M., and G. Iverson, 1993. Color constancy. I. Basic theory of two-stage linear recovery of spectral descriptions for lights and surfaces, *J. Opt. Soc. Am. A*, 10:2148–2165.

D'Zmura, M., G. Iverson, and B. Singer, 1995. Probabilistic color constancy. in *Geometric Representations of Perceptual Phenomena: Papers in Honor of Tarow Indow's 70th Birthday* (R. D. Luce, M. D'Zmura, D. Hoffman, G. Iverson, and A. K. Romney, eds.), Mahwah, NJ: Erlbaum, pp. 187–202.

D'Zmura, M., and P. Lennie, 1986. Mechanisms of color constancy, *J. Opt. Soc. Am. A*, 3:1662–1672.

D'Zmura, M., and A. Mangalick, 1994. Detection of contrary chromatic change, *J. Opt. Soc. Am. A*, 11:543–546.

Epstein, W., 1961. Phenomenal orientation and perceived achromatic color, *J. Psychol.*, 52:51–53.

Eskew, R. T., J. S. McLellan, and F. Giulianini, 1999. Chromatic detection and discrimination, in *Color Vision: From Molecular Genetics to Perception* (K. Gegenfurtner and L. T. Sharpe, eds.), Cambridge: Cambridge University Press, pp. 345–368.

Finlayson, G. D., M. S. Drew, and B. V. Funt, 1994. Color constancy—generalized diagonal transforms suffice, *J. Opt. Soc. Am. A*, 11:3011–3019.

Finlayson, G. D., P. H. Hubel, and S. Hordley, 1997. Color by correlation. Paper presented at the IS&T/SID Fifth Color Imaging Conference. Scottsdale, AZ: Color Science, Systems, and Applications.

Flock, H. R., and E. Freedberg, 1970. Perceived angle of incidence and achromatic surface color, *Percept. Psychophys.*, 8:251–256.

Foley, J. D., A. van Dam, S. K. Feiner, and J. F. Hughes, 1990. *Computer Graphics: Principles and Practice*, 2nd ed. Reading, MA: Addison-Wesley.

Forsyth, D. A., 1990. A novel algorithm for color constancy, *Int. J. Comput. Vis.*, 5:5–36.

Foster, D. H., and S. M. C. Nascimento, 1994. Relational colour constancy from invariant cone-excitation ratios, *Proc. R. Soc. Lond. B*, 257:115–121.

Funt, B. V., and M. S. Drew, 1988. Color constancy computation in near-Mondrian scenes using a finite dimensional linear model. Paper presented at the IEEE Computer Vision and Pattern Recognition Conference, Ann Arbor, MI.

Gelb, A., 1950. Colour constancy, in *Source Book of Gestalt Psychology* (W. D. Ellis ed.), New York: Humanities Press, pp. 196–209.

Gilchrist, A., and A. Jacobsen, 1984. Perception of lightness and illumination in a world of one reflectance, *Perception*, 13:5–19.

Gilchrist, A. L., 1977. Perceived lightness depends on perceived spatial arrangement, *Science*, 195:185.

Gilchrist, A. L., 1980. When does perceived lightness depend on perceived spatial arrangement? *Percept. Psychophys.*, 28:527–538.

Gilchrist, A. L., C. Kossyfidis, F. Bonato, T. Agostini, J. Cataliotti, X. Li, B. Spehar, V. Annan, and E. Economou, 1999. An anchoring theory of lightness perception, *Psychol. Rev.*, 106:795–834.

Golz, J., and D. I. A. MacLeod, 2002. Influence of scene statistics on colour constancy, *Nature*, 415:637–640.

Helson, H., and V. B. Jeffers, 1940. Fundamental problems in color vision. II. Hue, lightness, and saturation of selective samples in chromatic illumination, *J. Exp. Psychol.*, 26:1–27.

Helson, H., and W. C. Michels, 1948. The effect of chromatic adaptation on achromaticity, *J. Opt. Soc. Am.*, 38:1025–1032.

Hochberg, J. E., and J. Beck, 1954. Apparent spatial arrangement and perceived brightness, *J. Exp. Psychol.*, 47:263–266.

Hurlbert, A. C., 1998. Computational models of color constancy, in *Perceptual Constancy: Why Things Look as They Do* (V. Walsh and J. Kulikowrki, eds.), Cambridge: Cambridge University Press, pp. 283–322.

Hurlbert, A. C., H. Lee, and H. H. Bulthoff, 1989. Cues to the color of the illuminant, *Invest. Ophthalmol. Vis. Sci.*, Suppl., 30:221.

Hurvich, L. M., and D. Jameson, 1958. Further development of a quantified opponent-color theory, in *Visual Problems of Colour II*, London: HMSO, pp. 693–723.

Jaaskelainen, T., J. Parkkinen, and S. Toyooka, 1990. A vector-subspace model for color representation, *J. Opt. Soc. Am. A*, 7:725–730.

Jameson, D. B., and L. M. Hurvich, 1964. Theory of brightness and color contrast in human vision, *Vis. Res.*, 4:135–154.

Judd, D. B., D. L. MacAdam, and G. W. Wyszecki, 1964. Spectral distribution of typical daylight as a function of correlated color temperature, *J. Opt. Soc. Am.*, 54:1031–1040.

Kaiser, P. K., and R. M. Boynton, 1996. *Human Color Vision*, 2nd ed., Washington, DC: Optical Society of America.

Katz, D., 1935. *The World of Colour* (R. B. MacLeod and C. W. Fox, trans.), London: Kegan, Paul, Trench Truber and Co.

Khang, B. G., and Q. Zaidi, 2002. Cues and strategies for color constancy: perceptual scission, image junctions and transformational color matching, *Vis. Res.*, 42:211–226.

Knill, D. C., and D. Kersten, 1991. Apparent surface curvature affects lightness perception, *Nature*, 351:228–230.

Koffka, K., 1935. *Principles of Gestalt Psychology*, New York: Harcourt, Brace.

Kraft, J. M., and D. H. Brainard, 1999. Mechanisms of color constancy under nearly natural viewing, *Proc. Natl. Acad. Sci. USA*, 96:307–312.

Kraft, J. M., S. I. Maloney, and D. H. Brainard, 2002. Surface-illuminant ambiguity and color constancy: effects of scene complexity and depth cues, *Perception*, 31:247–263.

Krantz, D., 1968. A theory of context effects based on cross-context matching, *J. Math. Psychol.*, 5:1–48.

Krauskopf, J., D. R. Williams, and D. W. Heeley, 1982. Cardinal directions of color space, *Vis. Res.*, 22:1123–1131.

Land, E. H., 1959a. Color vision and the natural image, part I, *Proc. Natl. Acad. Sci. USA*, 45:116–129.

Land, E. H., 1959b. Color vision and the natural image, part II, *Proc. Natl. Acad. Sci. USA*, 45:636–644.

Land, E. H., 1986. Recent advances in retinex theory, *Vis. Res.*, 26:7–21.

Land, E. H., and J. J. McCann, 1971. Lightness and retinex theory, *J. Opt. Soc. Am.*, 61:1–11.

Larson, G. W., and R. Shakespeare, 1998. *Rendering with Radiance: The Art and Science of Lighting Visualization*, San Francisco: Morgan Kaufman.

Lee, H., 1986. Method for computing the scene-illuminant chromaticity from specular highlights, *J. Opt. Soc. Am. A*, 3:1694–1699.

Lennie, P., and M. D'Zmura, 1988. Mechanisms of color vision, *CRC Crit. Rev. Neurobiol.*, 3:333–400.

Maloney, L. T., 1986. Evaluation of linear models of surface spectral reflectance with small numbers of parameters, *J. Opt. Soc. Am. A*, 3:1673–1683.

Maloney, L. T., 1999. Physics-based approaches to modeling surface color perception, in *Color Vision: From Genes to Perception* (K. T. Segenburtned and L. T. Sharpe, eds.), Cambridge: Cambridge University Press, pp. 387–416.

Maloney, L. T., and B. A. Wandell, 1986. Color constancy: a method for recovering surface spectral reflectances, *J. Opt. Soc. Am. A*, 3:29–33.

Marr, D., 1982. *Vision*, San Francisco: W. H. Freeman.

McCann, J. J, 1994. Psychophysical experiments in search of adaptation and the gray world. Paper presented at the IS&T's 47th Annual Conference, Rochester, NY.

McCann, J. J., S. P. McKee, and T. H. Taylor, 1976. Quantitative studies in retinex theory: a comparison between theoretical predictions and observer responses to the "Color Mondrian" experiments, *Vis. Res.*, 16:445–458.

Mollon, J. D., in press. The origins of modern color science, in *The Science of Color*, 2nd ed. (S. K. Shevell ed.), Optical Society of America.

Pessoa, L., E. Mingolla, and L. E. Arend, 1996. The perception of lightness in 3-D curved objects, *Percept. Psychophys.*, 58(8): 1293–1305.

Poirson, A. B., and B. A. Wandell, 1993. Appearance of colored patterns—pattern color separability, *J. Opt. Soc. Am. A*, 10:2458–2470.

Rodieck, R. W., 1998. *The First Steps In Seeing*, Sunderland, MA: Sinauer.

Shevell, S. K., 1978. The dual role of chromatic backgrounds in color perception, *Vis. Res.*, 18:1649–1661.

Shevell, S. K., and J. Wei, 1998. Chromatic induction: border contrast or adaptation to surrounding light? *Vis. Res.*, 38:1561–1566.

Singer, B., and M. D'Zmura, 1995. Contrast gain control—a bilinear model for chromatic selectivity, *J. Opt. Soc. Am. A*, 12:667–685.

Stiles, W. S., and B. H. Crawford, 1932. Equivalent adaptation levels in localised retinal areas. Paper presented at the Report of Discussions of the Vision Physiology Society of London.

von Kries, J., 1905/1970. Influence of adaptation on the effects produced by luminous stimuli, in *Sources of Color Vision* (D. L. MacAdam ed.), Cambridge, MA: MIT Press.

Walraven, J., 1976. Discounting the background: the missing link in the explanation of chromatic induction, *Vis. Res.*, 16:289–295.

Webster, M. A., 1996. Human colour perception and its adaptation, *Network: Comput. Neural Syst.*, 7:587–634.

Webster, M. A., and J. D. Mollon, 1991. Changes in colour appearance following post-receptoral adaptation, *Nature*, 349:235–238.

Werner, J. S., and J. Walraven, 1982. Effect of chromatic adaptation on the achromatic locus: the role of contrast, luminance and background color, *Vis. Res.*, 22(8):929–944.

Yang, J. N., and L. T. Maloney, 2001. Illuminant cues in surface color perception: tests of three candidate cues, *Vis. Res.*, 41:2581–2600.

Zaidi, Q., 1998. Identification of illuminant and object colors: heuristic-based algorithms, *J. Opt. Soc. Am. A*, 15:1767–1776.

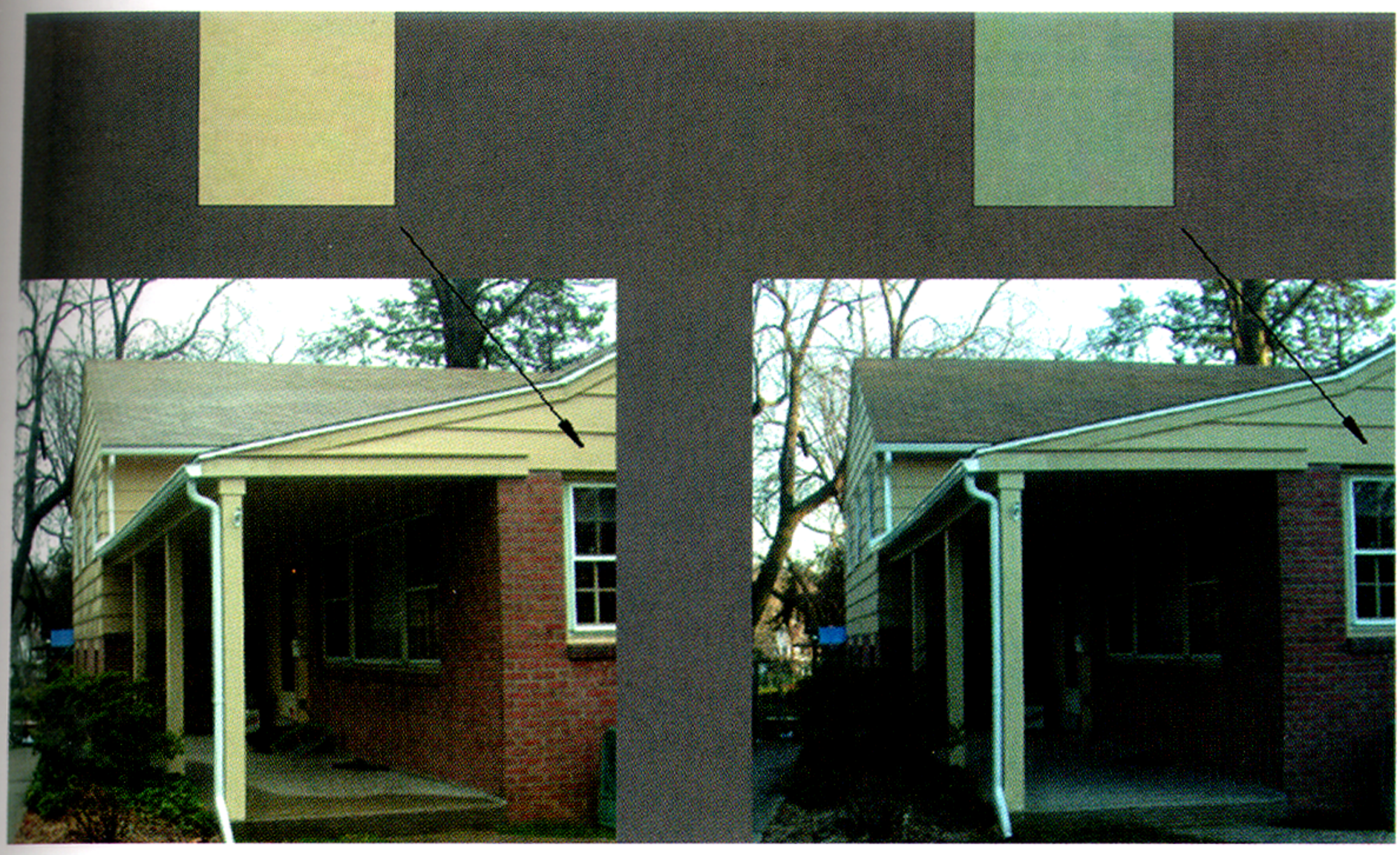

PLATE 36 Same objects imaged under two natural illuminants. *Top*: The patches show a rectangular region extracted from images of the same object under different outdoor illuminants. *Bottom*: The images from which the patches were taken. Images were acquired by the author in Merion Station, Pennsylvania, using a Nikon CoolPix 995 digital camera. The automatic white balancing calculation that is a normal part of the camera's operation was disabled during image acquisition. (See Fig. 61.1.)

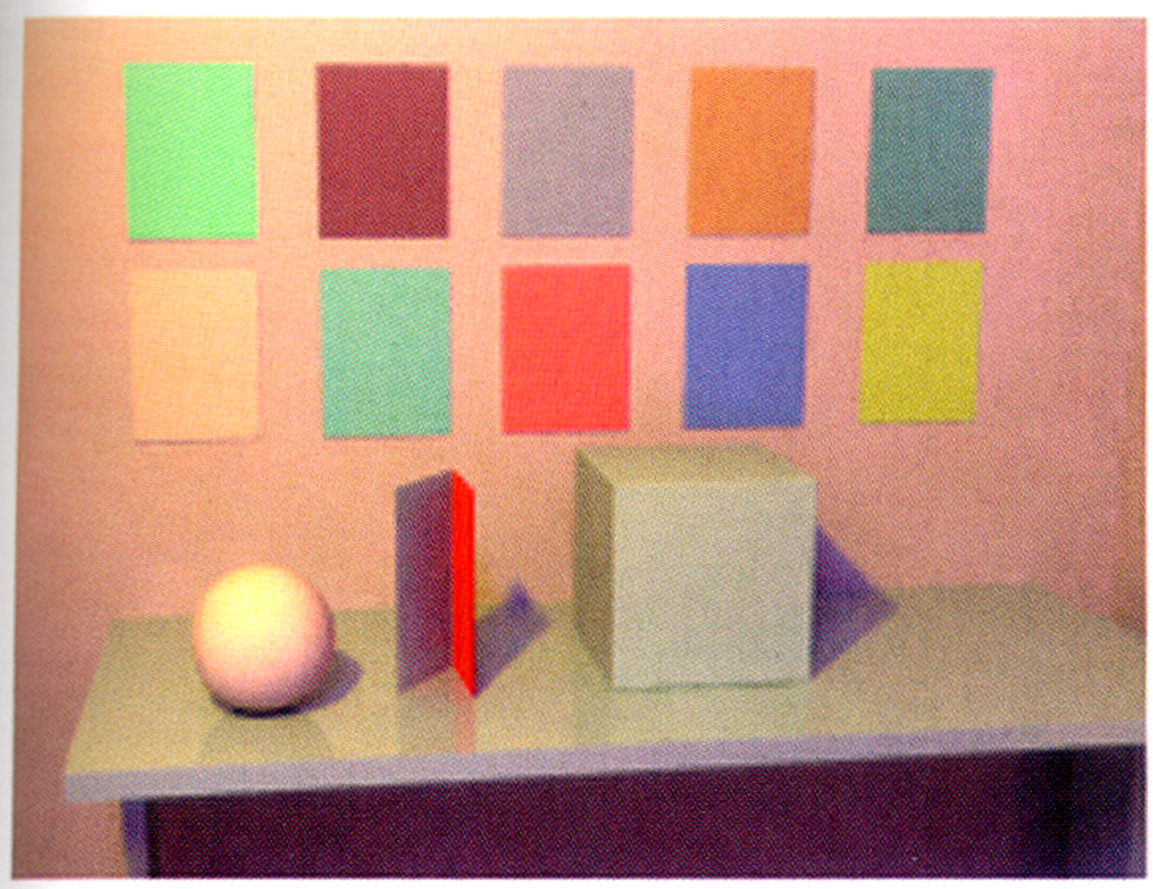

PLATE 37 Image formation. Each set of square patches around the side of the image illustrates variation in the light reflected to the eye when surface reflectance is held fixed. *Gradient*: The two patches shown were extracted from the upper left (L) and lower right (R; above table) of the back wall of the scene. *Shadow*. The two patches were extracted from the tabletop in direct illumination (D) and shadow (S). *Shape*: The three patches shown were extracted from two regions of the sphere (T and B; center top and right bottom, respectively) and from the colored panel directly above the sphere (P; the panel is the leftmost of the four in the bottom row). Both the sphere and the panel have the same simulated surface reflectance function. *Pose and indirect illum.* The four patches were extracted from the three visible sides of the cube (R, L, and T; right, left, and top visible sides, respectively) and from the left side of the folded paper located between the cube and the sphere (I). The simulated surface reflectances of all sides of the cube and of the left side of the folded paper are identical. The image was rendered from a synthetic scene description using the RADIANCE computer graphics package (Larson and Shakespeare, 1998). There were two sources of illumination in the simulated scene: a diffuse illumination that would appear bluish if viewed in isolation and a directional illumination (from the upper left) that would appear yellowish if viewed in isolation. All of the effects illustrated by this rendering are easily observed in natural scenes. (See Fig. 61.2.)

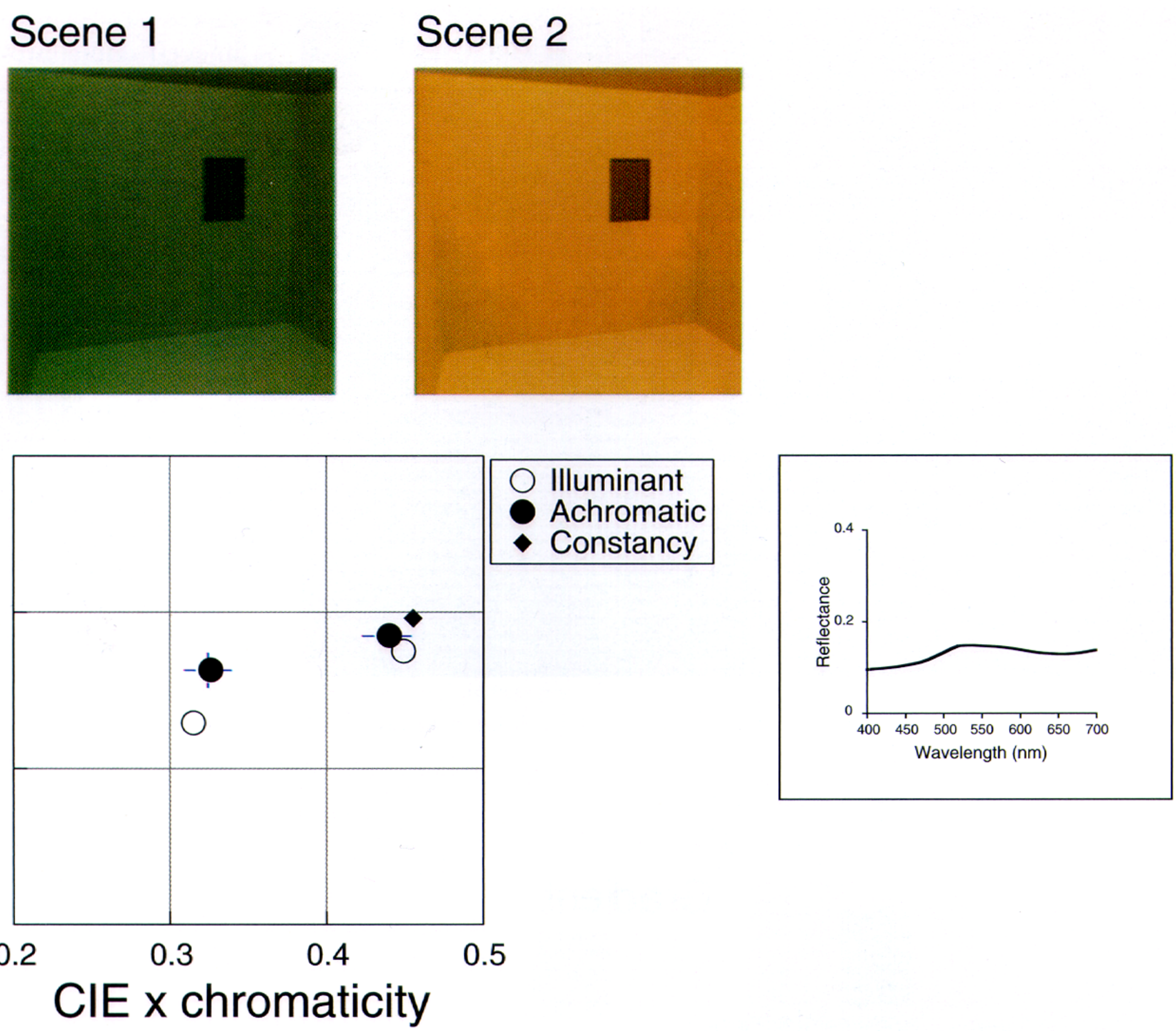

PLATE 38 Basic data from an achromatic adjustment experiment. The images at the top of the figure show the observer's view of two scenes, labeled 1 and 2. The test patch is visible in each image. The projection colorimeter was turned off at the time the images were acquired, so the images do not show the results of observers' achromatic adjustments. The chromaticity diagram shows the data from achromatic adjustments of the test patch made in the context of the two scenes. The open circles show the chromaticity of the illuminant for each scene. The illuminant for Scene 1 plots to the lower left of the illuminant for Scene 2. The closed circles show the chromaticity of the mean achromatic adjustments of four observers. Where visible, the error bars indicate ±1 standard error. The surface reflectance function plotted in the inset at the right of the figure shows the equivalent surface reflectance $\tilde{s}(\lambda)$ computed from the data obtained in Scene 1. The closed diamond shows the color constant prediction for the achromatic adjustment in Scene 2, given the data obtained for Scene 1. See the explanation in the text. (See Fig. 61.4.)

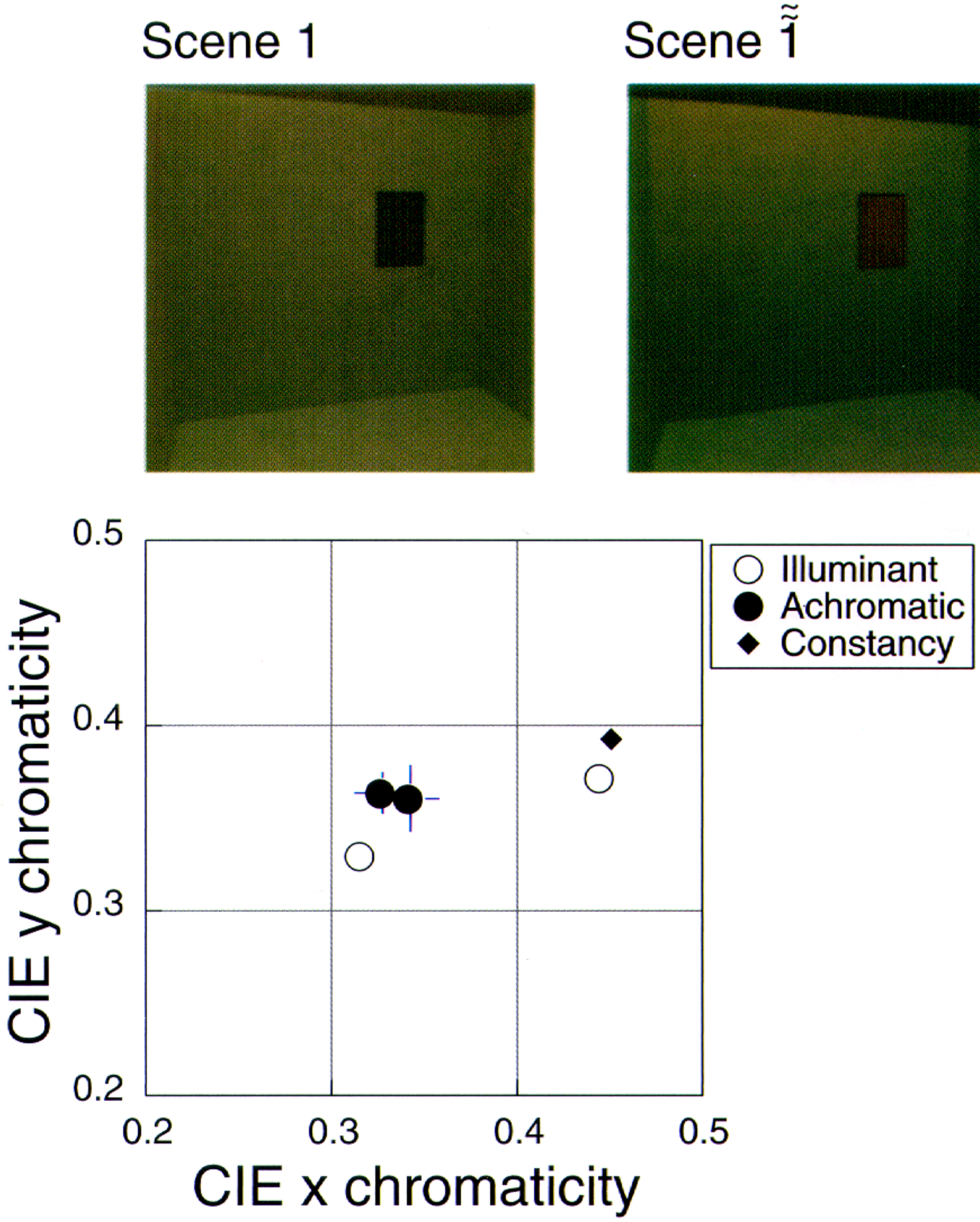

PLATE 39 Achromatic data when both illuminant and scene surfaces are varied. The images at the top of the figure show the observer's view of two scenes, labeled 1 and $\tilde{\tilde{1}}$. The relation between these scenes is described in the text. The test patch is visible in each image. The projection colorimeter was turned off at the time the images were acquired, so the images do not show the results of observers' achromatic adjustments. The chromaticity diagram shows the data from achromatic adjustments of the test patch made in the context of the two scenes. The format is the same as that of Figure 61.4. The equivalent surface reflectance $s(\lambda)$ computed from the data obtained in Scene 1 is shown in Figure 61.4. (See Fig. 61.6.)